AQUEOUS PHASE ABATEMENT OF PHENOL AND CADMIUM USING HYDROXYIRON (III) CALCINED WITH BENTONITE

Supported by
tetfund
TERTIARY EDUCATION TRUST FUND

R. Sha'Ato[1]*, G. O. Egah[1&2] and A. U. Itodo[1]
[1]Department of Chemistry, University of Agiculture Makurdi, Benue State, Nigeria
[2]Department of Pure & Applied Sciences, Federal University Wukari, Taraba State, Nigeria
*Corresponding author: rshaato@gmail.com

Received: January 20, 2018 **Accepted:** February 26, 2018

Abstract: In this study, Raw Bentonite (RB), Carbonized Bentonites(CB), Hydroxyiron (III) bentonite- composite (HBC), have been used for the adsorption of phenol and cadmium from aqueous solution. Effect of initial pH of adsorbates was carried out at pH 2-11 and adsorbent dosage from 0.5 to 2.5 g with 50 mL adsorbate solution. Adsorption thermodynamics were developed for 5-25 mg/L and 10-50 mg/L of phenol and cadmium solutions for 1 h. Adsorption experiments were performed for 1 h. RB, CB and HBC showed the following physicochemical characteristics: pH 7.38, 7.26 and 7.20; pHpzc: 11.00, 10.50 and 10.10; Conductivity (2μ/m):1.656, 1.660 and 1.657; Bulky density (g/cm^3):1.186, 1.111 and 1.214; Attrition (%): 17.49, 26.53 and 27.21, respectively. Adsorbent features were determined using XRF, FTIR and SEM techniques. The presence of hydroxyl, carboxylic, hydrogen bonding and aldehyde group showed that adsorbents bonds phenol and cadmium. At equilibrium, the maximum adsorption efficiencies for phenol: RB (52.020%), CB (63.468%), HBC (79.952%) and cadmium: RB (41.980%), CB (48.398%), HBC (65.830%) respectively were achieved for contact time. Adsorption capacities were found to increase with increase in contact time, temperature and concentration. The equilibrium adsorption data fitted better into the Langmuir than the Freundlich model. Thermodynamic parameters – Gibbs energy, enthalpy and entropy change indicated that adsorption was endothermic, meaning that chemisorption dominates physisorption. Adsorption kinetics was better explained by the Blanchard pseudo-second order kinetic model than the Lagergren first order. Overall, the adsorption of phenol was more favourable than for cadmium for all adsorbents.

Keywords: Adsorption, bentonite, phenol, cadmium, kinetic, thermodynamic

Introduction

Environmental contamination by phenol and cadmium (Cd) has become an important issue due to the potential hazard both pollutants pose to living organisms. As a result a lot of efforts have been devoted to minimize the harmful effects of these pollutants to plants, animals and humans (Moradi *et al.*, 2015). Specifically, the presence of phenol in waste water has become a major source of concern to environmentalist because for it is considered as toxic, hazardous and priority pollutant (Afaj *et al.*, 2015). The wastewaters discharged from pesticide, soap, paint, solvent, pharmaceuticals, and paper and pulp industries and also water disinfecting process constitute a major source of phenol in wastewaters (Bhole *et al.,* 2004). Phenol is water soluble and highly mobile and small amount may cause severe diseases like cancer, nausea, vomiting, paralysis, smoky colored urine (Afaj *et al.*, 2015). The maximum permitted concentration level of phenol according to US Environmental Protection Agency (EPA) is 0.5-1 mg/L for industrial wastewater and 1μg/L for drinking water (Afaj *et al.*, 2015).

On the other hand, Cadmium has been reported to cause health problems due to its high toxicity, non-biodegradable and bio-accumulation in living organisms (Dawodu *et al.*, 2012). The sources (Bhole *et al.*, 2004), toxicity (Ahmed *et al.*, 2015). And adverse (Srivastava *et al.*, 2006) has been documented.

Rao *et al.*, (2011) reviewed various methods for the removal of water pollutants such as chemical precipitation, ion exchange, reverse osmosis, electro-dialysis, ultra-filtration, nano-filtration, coagulation, flocculation, floatation, membrane filtration, biological oxidation, solvent extraction, complexing, ion exchange and adsorption.

Adsorption is one of the physicochemical treatment processes used for pollutant removal due to their low cost and high efficiency (Arellano-C'Ardenas *et al.*, 2005). Bentonites are good absorbents used in adsorption due to their large surface area, ion-exchange capacity, adsorption, high versatility, easily manipulated properties, and low costs materials in water pollution remediation processes (Bhattacharya *et al.*, 2014). This research is aimed at developing a low cost adsorbent for the removal of Cadmium and Phenol using Hydroxyiron (III) ($Fe(OH)_3$) calcined with Bentonite. Batch adsorption technique was applied and the effect of such factors as initial pH, adsorbent dosage, initial concentration, contact time and temperature was investigated. To help the description of the adsorption process, equilibrium isotherm models were applied.

Adsorption isotherms

Langmuir isotherm: This is based on assumptions that the maximum adsorption occurred due to a saturated mono-layer of adsorbate molecules on the adsorbent surface (Li *et al.*, 2005). According Chen, (2015), the Langmuir adsorption isotherm is expressed as Equation 1.

$$\frac{1}{Q_e} = \frac{1}{Q_m} + \frac{1}{C_e} \times \frac{1}{bQ_m} \qquad (1)$$

Where Q_m **(mg/g)** is the total number of binding sites that are available for sorption, C_e is the equilibrium concentration of the solute in the bulk solution (mg/L), Q_e (mg/g) is the amount of solute sorbed per unit mass of the adsorbent at equilibrium and b (L/mg) is the Langmuir constant for the Adsorbate-Adsorbent. The higher the magnitude of b, the higher the heat of sorption and the stronger the bond formed.

A linear plot of $1/Q_e$ versus $1/C_e$ gives a straight line, with the slope and the intercept of $1/Q_m$ and $1/bQ_m$, respectively. The characteristics of the langmuir isotherm are determined by the dimensionless constant called separation factor, R_L expressed as Equation 2.

$$R_L = \frac{1}{(1+R_{L}C_0)} \qquad (2)$$

Where R_L (L/mg) and C_0 (mg/L) retained their usual meaning as stated earlier. R_L indicates the nature of adsorption process shown as: $R_L > 1$, is unfavourable, $R_L = 1$ is linear, R_L between 0 - 1 is favourable and $R_L = 0$ is irreversible (Krishna and Swamy, 2012).

Freundlich isotherm: The Freundlich isotherm is based on multilayer adsorption on the heterogeneous surface of the adsorbent containing an unequal amount of energies (Bansal and Goyal, 2005). It is used for both monolayer multi-layer adsorption. The linear equation of Freundlich isotherm as adopted by Krishna and Swamy (2012) is given as Equation 3.

$$logQ_e = \frac{1}{n_f} logc_e + logK_f \qquad (3)$$

Where Q_e (mg/g) is the amount of adsorbate that is adsorbed per unit mass of the adsorbent and C_e (mg/L) is the equilibrium concentration. K_f is the Freundlich constants related to the adsorption capacity and n_f is the adsorption intensity (Bansal and Goyal, 2005). A linear plot of $logQ_e$ versus $logC_e$ gives the slope of n_F and intercept K_f. If the value of n lies in the range of 1 to 10, they are classified as good adsorption according to Freundlich as reported by Krishna and Swamy (2012).

Adsorption kinetics

Chemical kinetics deals with the experimental conditions influencing the rate of a chemical reaction. Herein, two kinetic models including the pseudo-first-order and pseudo-second-order were used to analyze the experimental data and model of the adsorption process (Essomba *et al.*, 2014).

Pseudo first order model

Pseudo first order is most time used for adsorbate - adsorption in liquid- solid phase adsorption experiment (Ajay *et al.*, 2015). The Lagergren first-order equation as adopted by El-Dars *et al.* (2016) is as expresses as Equation 4.

$$\log(Q_e - \log Q_t) = logQ_e - \frac{K_1}{2.303} t \qquad (4)$$

Where Q_t is the amount of adsorbate adsorbed per unit of adsorbent (mg/g) at contact time t (min), Q_e is the amount of adsorbate adsorbed per unit mass of the adsorbent in (mg/g), k_1 is the pseudo first order rate constant (L/min). A linear plot of $\ln(Q_e - Q_t)$ versus t gives k_1 as the rate constant, $-\frac{K_1}{2.303}$ as the slope and log Q_e as the intercept (El-Dars *et al.*, 2016).

Blanchard pseudo-second order model

Pseudo second order was presented Bai *et al.*, (2010) and expressed as Equation 5.

$$\frac{t}{Q_1} = \frac{1}{K_2 Q_{e^2}} + \frac{1}{Q_e} t \qquad (5)$$

Where: K_2 is the pseudo-second rate constant ($g.mg^{-1}.min^{-1)}$ and the initial adsorption rate, h(mg/g.min) = $K_2 Q_e^2$. A linear plot of $\frac{t}{Q_t}$ versus t gives us K_2 the second- order rate constant, $\frac{1}{Q_e}$ as the slope and $\frac{1}{K_2 Q_{e^2}}$ as the intercept (Bai *et al.*, 2010)

Adsorption thermodynamics

The thermodynamics of adsorption was applied to obtain important parameters such as free energy change ΔG^0 in ($kJmol^{-1}$), enthalpy change ΔH^0 in ($kJmol^{-1}$) and the entropy change ΔS^0 in ($JK^{-1}mol^{-1}$) which helps which helps provide a better understanding of the adsorption process (Dawodu *et al.*, 2012). The thermodynamics equation as adopted by Jameel *et al.* (2012) was given as Equation 6.

$$\log(\frac{q_e}{C_e}) = \frac{\Delta S^\circ}{2.303R} - (\frac{\Delta H^\circ}{2.303R}) \frac{1}{T} \qquad (6)$$

Where Q_e/C_e is the adsorption affinity, R is the universal gas constant (8.314 $Jmol^{-1}K^{-1}$) T is the temperature in (K). The thermodynamic parameters were calculated from the plot of log (qe/C_e) versus $1/T$ which give a straight line graph where – (ΔH^0/2.303R) is the slope and (ΔS^0/2.303R) is the intercept and the free Gibbs energy is given as calculated as Equation 7.

$$\Delta G^\circ = \Delta H^\circ - T\Delta S^\circ \qquad (7)$$

Where T is the standard temperature (298 K)

Methods

Sampling and sample identification

The raw Bentonite used in this work was supplied by Knexel Nigeria Limited, no; 27, Adeleke Street, Ikeja, Lagos State, Nigeria. The samples were taken for proper identification in the Department of Soil Science, Federal University Wukari, Taraba State.

Preparation of the adsorbents

Hydroxyiron (III) $Fe(OH)_3$ was prepared by reaction of an anhydrous ferric chloride ($FeCl_3$) solution with Sodium Hydroxide NaOH solution which leads to a formation of precipitate. The precipitate was filtered using filter paper, dried in an oven for about 24 hrs and crushed into powder. Finally, it was stored as $Fe(OH)_3$ in an air tight container for future use. The equation of reaction is shown as Equation 8.

$$FeCl_{3(aq)} + 3NaOH_{(aq)} \rightarrow Fe(OH)_{3(s)} + 3NaCl_{(aq)} \qquad (8)$$

For the preparation of raw bentonite (RB), 3 kg of the raw bentonite was washed thoroughly with distilled water in order to remove any dissolved impurities, dried in an oven at 110°C for 2 h and crushed and sieved using vibrator sieve shaker to determine the particle size (63 µm) (Karapinar and Donat, 2009). The raw bentonite was stored as RB in an air tight container for future use. One (1) kg of the raw bentonite was calcined in a muffle furnace at 600°C for 1 h. It was then cooled and sealed in an air tight container as CB which was used as control. The composite was prepared by mixing the hydroxyiron (III) ($Fe(OH)_3$) prepared with raw bentonite at ratio 3:1 and calcined in muffle furnace at temperature of 600°C for 1 h. Finally, the modified adsorbent was stored in an air tight container as HBC for future use. The adsorbent yield was computed from Equation 9.

$$\%\boldsymbol{yield} = \frac{weight\ of\ calcined}{weight\ of\ raw\ material} \times 100 \qquad (9)$$

Characterization of adsorbents

pH: The pH of the adsorbents was determined by method adopted by Kibami *et al.* (2014). A 1.0 g of the absorbent was weighed into 100 mL distilled water in a beaker and kept on a magnetic stirrer for 1hour at 120 rpm. The pH was then measured and recorded. The pH readings were taken in triplicates using HI 8014 pH meter (Hanna instruments).

Point zero charge (pH_{PZC}): pHzpc of an adsorbent is important because it indicates the net surface charge of the adsorbent in solution (Kosmulski, 2009). The pHzpc was determined by methods adopted by Kibami *et al.* (2014). The pHzpc is the point where the curve of pH (final) vs pH (initial) intersects the line pH (initial) = pH (final). In order to determine the pH of point of zero charge 0.5 g of the adsorbent was added to buffer solution of different pH's ($pH_{Initial}$) values of 4, 7 and 10. This was shaked for 2 h and measured as $pH_{Final.}$ A relation of $pH_{Initial}$ on X-axis and pH_{final} – $pH_{initial}$ on Y-axis was plotted. The intercept of X-axis was taken as the point zero charge.

Conductivity (µS/m) of adsorbents: Conductivity was measured using method adopted by Bansode, (2002). A 1.0 g of the adsorbent was suspended in distilled water for 20 minutes and its conductivity measured in two micro-Siemen (2 µS) using DDS-307 Conductivity meter (Pec Medicals USA).

Bulk density: The bulk density was determined using the tamping method of Ahmedna *et al.* (2000). A 5 g portion of each adsorbent was packed in a 10ml measuring cylinder to a specified volume and tapped until it occupied a minimum volume. The apparent volume is read to the nearest graduated unit. The bulk density was measured using Equation 10.

$$Bulk\ density\ (g/cm^3) = \frac{Mass\ of\ the\ adsorbent\ (g)}{Apparent\ Volume\ of\ adsorbent (cm^3)} \qquad (10)$$

Attrition/Hardness (%): Attrition or hardness is the measure of the mechanical strength and it is an important parameter used to determine the adsorbent ability to withstand normal handling operations. The attrition of the samples was measured using wet attrition method described by Toles *et al.* (2000). A 1.0 g of the adsorbent was added to 100 ml of distilled water. The solution was stirred at 200 rpm for 2 h using magnetic stirrer. The solution was then filtered using filter paper and the retained adsorbent was dried at room temperature. The % attrition was measured using Equation 11.

$$Attrition\ (\%) = \frac{Initial\ mass(g) - Final\ mass(g)}{Initial\ mass(g)} \times 100 \quad (11)$$

Batch adsorption experiment

Several standard concentrations (10, 20, 30, 40 and 50 mg/L) of cadmium and (5, 10, 15, 20 and 25 mg/L) of phenol were prepared from the standard 1000 and 100 mg/L stock solution, respectively.

The pH adjustment was done by drop-wise addition of 0.1 M NaOH and 0.1 M HCl with the aid of a Hanna digital pH meter until the desired value was obtained. In the batch adsorption experiment, 0.5 g of each adsorbent was contacted with 50 ml of known concentration adsorbate solution in conical flask (250 ml) in capacity, and stirred for (60 minute) constant contact time by mechanical shaker at (200 rpm) at room temperature until equilibrium was achieved. At the end of the contact time required, the solution was filtered using filter paper and the filtrate analyzed for residual adsorbate concentrations for Phenol using UV-visible spectrophotometer at a maximum wavelength of 270 nm (Shimadzu, UV-1700 spectrophotometer) and atomic adsorption spectrophotometer (AAS) for Cadmium at 228.8 nm.

Batch adsorption experiments were performed by varying the pH, Adsorbent dosage, concentration, Contact time and Temperature. The effect of pH was performed in the range pH (2 – 11), adsorbent dosage in the range of 0.5-2.5 g, initial phenol and Cadmium ion concentration in the range 5-25 mg/L and 10-50 mg/L, respectively; contact time of 10 - 60 min was used to determine the equilibrium time and Temperature of range 25-55°C. In each case the parameter to be studied was varied while other parameters were kept constant. This was done for each experiment in a particular study, the experiment was repeated in each case and the mean value was calculated to minimize errors. In all batch adsorption experiment, the amount of Phenol and Cadmium, Q_e (mg/g), was calculated by the mass balance Equation (14) adopted by Kibami *et al.* (2014)

$$Q_{e\,(mg/g)} = \frac{(C_o - C_e)}{M_a} v \quad (14)$$

Where Q_e represent the adsorption capacity, C_o and C_e are the initial and residual Phenol and Cadmium concentrations (mg/L), respectively; *V* was the aliquot volume of Phenol and Cadmium solution in (L) used and m_a the mass of adsorbent in (g) used for a particular batch treatment. The percentage removal of phenol and Cadmium were calculated using Equation 15.

$$\%\ Removal = \frac{(C_o - C_e)}{C_o} \times 100 \quad (15)$$

% Removal is also called adsorption efficiency

Results and Discussion

Physicochemical attributes of adsorbents

pH gives an idea of the acidic and basic nature of an adsorbent which determines the effect on the surface charge of the adsorbent and on the degree of ionization of adsorbate (Bousba and Meniai, 2013). From the result in Table 1, the pH of RB, CB and HBC were found to be (7.38, 7.26 and 7.20) respectively indicating that all the adsorbents are neutral. According to Okieimen and Okieimen (2001), adsorbents with pH in the range of 6-8 are good for adsorption. It implies that the adsorbents have good pH for adsorption.

pHpzc gives an idea of the surface charge of an adsorbent which is an important indication in adsorption (Tan *et al.*, 2012). In general, if pHpzc > pH, the surface of the adsorbent would be positively charged, and the repulsive force would result in a decrease of adsorption and vice versa favours adsorption (Tan *et al.*, 2012). Table 1 shows the point zero charge (pHpzc) of the various adsorbents (RB, CB and HBC) were found to be 11.00, 10.50 and 10.10, respectively, showing that their pH at zero point charges are above 7.0 for all the samples. This is an indication of positively charged surface, which arises from the basic sites that combine with protons from the medium. Similar results were reported by Kibami *et al.*, (2014) studies on the Preparation and characterization of activated carbon from *Fagopyrum esculentum* Moench by HNO_3 and H_3PO_4 chemical activation.

Conductivity gives an idea of the amount of charges on the surface (Bansode *et al.*, 2002). Result from Table 1, the conductivity of RB, CB, and HBC at two micro Siemen's (2µS/m) were found to be (1.656 µS/m, 1.660 µS/m and 1.657 µS/m) respectively. According to Bansode (2002), high conductivity of the adsorbent is undesirable as it interferes in the adsorption process because of the leachable minerals associated to the adsorbent surface. This implies that all the adsorbents have good conductivity for adsorption process since they all have low value of conductivity.

Bulk density (g/cm^3) gives an estimate of packing volume of an adsorbent which is an important parameter in adsorbate uptake (Kibami *et al.*, 2014). The lower the bulk density values, the better its ability for regeneration upon use (Abdus-Salam and Buhari, 2014). From the result in Table 1, values of Bulk density for RB, CB and HBC were found to be (1.186, 1.111 and 1.214 g/cm^3), respectively. These bulk densities are above 1 g/cm^3 which agrees with the values reported by Krishna and Swamy., 2012 (1.3207 g/cm^3) which suggested that all the adsorbent have good densities for adsorption.

Attrition is an important parameter for understanding the relative percentage loss of an adsorbent during transportation, stirring and regeneration (Bansode, 2002). From the results in Table 1, the percentage Attrition for RB, CB and HBC were found to be (17.49, 26.53 and 27.21%) which are lower compared to those obtained by Bansode (2002) from acid-activated almond shell based carbon ALA (31.68%). This implies that the adsorbents are good for adsorption since they are less susceptibility to abrasion losses during commercial utilization as compared to the values reported from acid-activated almond shell based carbon.

Table 1: Selected Physicochemical Attributes of Adsorbents

Parameters	RB	CB	HBC
Ph	7.38	7.26	7.20
pH$_{PZC}$	11.00	10.50	10.10
Conductivity (2µ)	1.656	1.660	1.657
Bulk-density (g/cm^3)	1.186	1.111	1.214
Attrition (%)	17.49	26.53	27.21

FTIR analysis of adsorbents

The FT-IR was also carried out using the KBr disk method (Johari *et al.*, 2014). The FTIR spectrum is important in identification of surface functional groups which could play a great role in adsorption mechanism and capacity (Kibami *et al.*, 2014). The FT-IR analysis of adsorbents is shown in Table 2.

For the FT-IR analysis of $Fe(OH)_3$, in Fig 4a. The peaks at 3850.04, 3726.60, 3595.43, and 3286.81 cm^{-1} within the frequency range of (3000-4000 cm^{-1}) are due to stretching vibrations of O-H groups. The band at 3850.04 and 3726.60

cm^{-1} is as a result of –OH groups sitting at the edge of the Fe(OH)$_3$ platelets (Ahmed *et al.*, 2015). The band at 3595.43 cm^{-1} is connected with the internal -OH stretching from hydroxyl groups which is in a range of 3620 cm^{-1} results obtained by Mohammad *et al.* (2010). The band at 3286.81 cm^{-1} represents the presence of –OH group (Ahmed *et al.*, 2015). The peak at 1527.67 cm^{-1} is attributed to the formation of oxygen functional groups such as a highly conjugated C-O stretching in carboxylic groups which is close to the 1535 cm^{-1} result obtained by Makeswari *et al.* (2016). 1257.63 cm^{-1} is C–O from acid and the peak at 1049.31 cm^{-1} is attributed to C-O stretch from alcohols. Similar results were reported by Gupta and Nayak (2011) studies on Cadmium removal and recovery from aqueous solutions by novel adsorbents prepared from orange peel and Fe$_2$O$_3$ nanoparticles.

Figure 4b shows the FTIR spectrum for raw bentonite. FTIR analysis of raw bentonite in the 3000-4000 cm^{-1} frequency range, shows bands at 3626.00 cm^{-1} and 3438.00 cm^{-1} which are attributed to the stretching vibrations of -OH groups (Ahmed *et al.*, 2015). This suggests that the adsorption may have been done on the OH bending of water, the inner surface -OH stretching vibration (Jiang *et al.*, 2011) and the Si–O bond linkage in bentonite (El-dars *et al.*, 2016). The sharp peak at 1648.53 cm^{-1} (ranging from 1620-1680 cm^{-1}) for the raw bentonite, is attributed to -OH bend vibration (Faye *et al.*, 2014). The band at 1028.00 cm^{-1} is ascribed to Si–O in-plane stretching vibration of Silica (El-dars *et al.*, 2016). The band at 918.91cm^{-1} is attributed to the bending Al-O-H vibrations of hydroxyl groups sitting on the alumina faces of the raw bentonite (Liew *et al.*, 2012). The bands at 784.66 cm^{-1} is attributed to Si-O stretching from Silica and 684.09 cm^{-1} is attributed to -OH symmetric stretching vibration (Liew *et al.*, 2012). The band at 531.00 cm^{-1} is due to Al^{4+}-O-Si vibrations, where Al^{4+} is in octahedral coordination (Liew *et al.*, 2012). Lastly, the band at 460.73 cm^{-1} is attributed the bending Si-O-Si vibrations (Liew *et al.*, 2012).

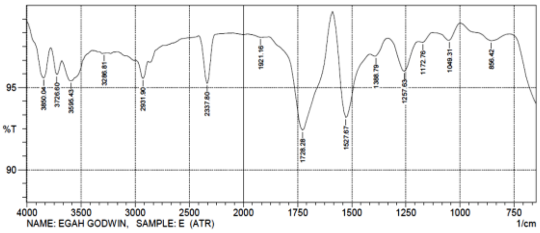

Fig. 4a: FTIR spectrum of hydroxyiron (III)

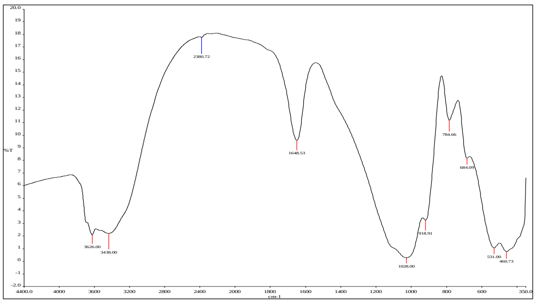

Fig. 4b: FTIR spectrum of raw bentonite (RB)

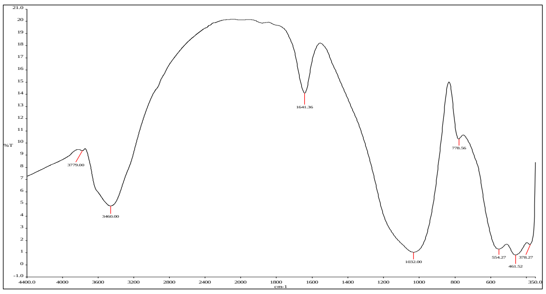

Fig. 4c: FTIR spectrum of hydroxyliron (iii) - bentonite composite (HBC)

The FT-IR spectrum in Figure 4c, of HBC has similar characteristics. The broad peak at 3779.00 and 3460.00 cm^{-1} (ranging from 3000-4000 cm^{-1}) are attributed to –OH group stretch from alcohol (Ahmed *et al.*, 2015). This suggests that the adsorption may have been done on the -OH bending of water, the inner surface -OH stretching vibration and the Si–O bond linkage in the hydroxyiron (III) - bentonite composite (El-dars *et al.*, 2016). The observed sharp peak at 1641.36 cm^{-1} (ranging from 1620-1680 cm^{-1}) for the hydroxyiron (III) – bentonite composite, is attributed to -OH bend vibration (Faye *et al.*, 2014). The broad tongue-like band at 1032.00 cm^{-1} is attributed to Si–O in-plane stretching vibration from Silica (El-dars *et al.*, 2016). The broad band at 778.56 cm^{-1} is attributed to Si-O stretching vibration (Arias and Sen, 2009). The band at 554.27 cm^{-1} is due to Al^{4+}-O-Si vibrations, where Al^{4+} is in octahedral coordination (Liew *et al.*, 2012). The band at 461.52 and 378.27 cm^{-1} are attributed to the bending of Si-O-Si vibrations (Aroke *et al.*, 2013).

Table 2: FT-IR analysis of adsorbents

Group Freq (cm^{-1})	Functional groups	Fe(OH)$_3$	RB	HBC	Assignment
4000-3000	Alcohol/Phenol	3850.04	-	-	Free OH stretch
	Alcohol/Phenol	3726.60	-	3779.00	O-H stretch
	Alcohol/Phenol	3595.43	3626.00	-	O-H stretch
	Alcohol/Phenol	-	3438.00	3460.00	-OH stretch
1680–1620	Alkenes	-	1648.53	1641.36	O-H Bend vibration
1550–1475	Carbonyl	1527.67	-	-	C-O stretch
1350-1100	Carbonyl	1257.63	-	-	C-O bend
1035-1050	Alcohol	1049.31	1028.00	1032.00	Si-O stretch
950–910	carboxylic acid	-	918.91	-	O-H bend
900 – 670	Aromatic	-	784.66	778.56	Si-O stretching vibration
	Phenol	-	684.09	-	O-H stretching vibration
500-300	Alkyl halides	-	531.00	554.27	Al-O-Si vibration
	Alkyl halides	-	460.73	461.52	Si-O-Si deformation
	Alkyl halides	-	-	378.27	Si-O-Si vibrations

RB = Raw Bentonite, HBC = Hydroxyliron (III) Bentonite Composite, RK = Raw Kaolin, HKC = Hydroxyliron (III) Kaolin Composite.

Table 3: Chemical composition of the adsorbents using XRF analysis

OXIDE	Al$_2$O$_3$	SiO$_2$	P$_2$O$_5$	SO$_3$	K$_2$O	CaO	MnO	Fe$_2$O$_3$	ZnO	SnO$_2$	Sb$_2$O$_3$	Total
RB (wt %)	17.05	58.01	0.36	2.54	1.51	0.12	0.04	17.97	0.09	0.90	0.86	99.45
HBC (wt %)	13.10	32.98	1.14	21.39	1.63	0.14	0.05	28.13	0.10	0.72	0.63	100

XRF characterization of adsorbents

Sky-ray Instrument (EDX3600B) X-ray fluorescence was used to analyze the chemical composition of raw bentonite.

Results are as presented in Table 3 for raw bentonite (RB) and Hydroxyiron (III) - bentonite composites (HBC). The XRF analysis performed using a voltage of 40 kv and 350 µA current shows that, the main constituents of RB were SiO_2 (58.0120 %), Al_2O_3 (17.0527 %) and Fe_2O_3 (17.9689 %) while other elements present in small amounts were P_2O_5 (0.3618 %), SO_3 (2.5434 %), K_2O (1.5043 %), CaO (0.1171 %), MnO (0.0420 %), ZnO (0.0903 %), SnO_2 (0.8997 %) and Sb_2O_3 (0.8619 %). It is thus expected that Phenol and cadmium ions in solution should be removed mainly by SiO_2 and Al_2O_3 (Dawodu *et al.,* 2012). Similar observations were reported by Dawodu *et al. (*2012) studies on isotherm modeling on the equilibrium sorption of Cadmium (II) ion from Solution by Agbani Clay.

For the XRF analysis of HBC, it is observed that the main constituents were SiO_2 (32.9828 %), Al_2O_3 (13.0992 %), SO_3 (21.3948 %) and Fe_2O_3 (28.1288 %). While other elements present in small amounts were P_2O_5 (1.1369 %), K_2O (1.6250 %), CaO (0.1420 %), MnO (0.0439 %), ZnO (0.1026 %), SnO_2 (0.7168 %) and Sb_2O_3 (0.6271 %). The reduction in percentage weight of SiO_2 and Al_2O_3 may be due to decomposition of impurities present in the sample during Calcination at 600^{o}C for 1 h (Ahmed *et al.,* 2015). While the increase in percentage weight of SO_3 and Fe_2O_3 may be due to addition of hydroxyiron (III) to bentonite. Similar observations were reported by Syafalni *et al.,* (2013).

Scanning electron microscopy analysis of adsorbents

Scanning electron microscope (SEM - JEOL, JSM 7600 F) was used to determine the surface morphology of the adsorbent. The sputter coater (Eiko IB-5 Sputter Coater) was operated in an argon atmosphere using a current of 6 mA for 3 min. SEM results shows an indication of pore development and occupation by adsorbates (Naswir *et al.,* 2013). Plates 1 – 3 show the micrograph of RB, CB and HBC. From the result in Plate 1, it is observed that the raw bentonite (RB) adsorbents showed a loose aggregate, uniform size and with porous structure. From Plate 2, it is observed that the Carbonized bentonite (CB) have a compact, fine particle, mono-disperse and had a mean diameter of 25–29 nm Mohammad *et al.* (2010).

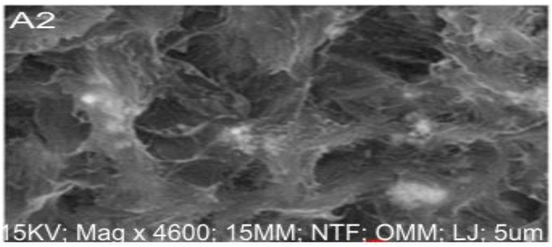

Plate 1: SEM Image of RB

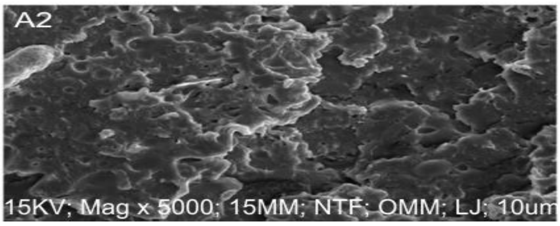

Plate 2: Scanning Electron Microscope (SEM) of CB

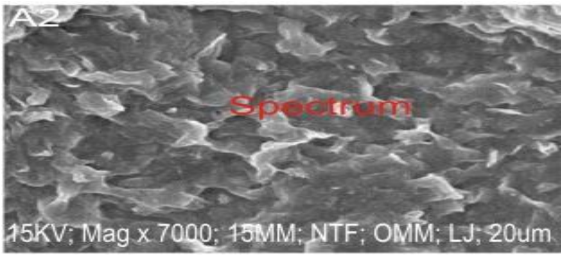

Plate 3: SEM Image of HBC

Plate 3, for hydroxyiron (III) bentonite composite (HBC) showed a porous, rough and irregular surface with crystalline structure which indicated more macro-pores for adsorption. Similar observation was reported by Ajay *et al.* (2015). Comparatively with the raw bentonite (RB) and Carbonized bentonite (CB), it can be concluded that the hydroxyiron (III) - bentonite composite (HBC) provides an external surface of porous and more reactive sites, which enhanced its adsorption capacity. Similar results were reported by Moradi *et al.* (2015).

Effect of adsorption experiment pH on adsorption of phenol and cadmium

Figures 5a shows the effect of pH on adsorption of phenol. Results shows the highest percentage removal for RB to be 54.528% at pH of 9, CB to be 53.432% at pH 7 and HBC to be 56.096% at pH of 7. From the result for all the adsorbents it was observed that optimum removal was achieved between pH 7-9 which may be due to increase in electrostatic attraction between the adsorbate and adsorbents (Bolat *et al.,* 2010). The ionization degree of phenol depends on the pH values of the solution (Mohanty *et al.,* 2005). At pH of 7- 9, phenol dissociate into negatively charge species such as the phenolate ($C_6H_5O^-$), which could be easily adsorbed on positively charged surfaces of adsorbents. A similar result was reported by (Allinor and Nwachukwu, 2012). The optimum pH for adsorption of phenol onto silicate was between pH 7-9. However, a decrease was observed as the pH approaches the alkaline condition at 11 from 54.528 -24.264%, 53.432 - 34.144% and 56.096 - 40.728% for RB, CB and HBC respectively which may be due to electrostatic repulsion between the anion and adsorbent as a result of decrease in negative charges at the phenolate surface in alkali pH (Denizli *et al.,* 2001). Hence, with increase of pH values, the adsorption efficiency decreased. Similar trend was also observed elsewhere (Nassef and Eltaweel *et al.,* 2012) for phenol removal from aqueous solutions using bentonite.

Results for Cadmium given in Figure 5b, pH was optimum at 2 for all the adsorbents. Result shows the highest percentage removal for RB to be 46.986%, CB to be 51.970% and HBC to be 75.980%. But increasing the pH from 2 – 11 brings about a decrease in percentage removal from 46.986 - 35.800%, 51.970 - 40.480% and 75.980 - 57.754% for RB, CB and HBC, respectively. The increase in adsorption with pH can be explained that acidic pH favors cation exchange that occurs between the adsorbents and the adsorbate (Dawodu *et al.,* 2012). At low pH values the solution is strongly acidic and a lot of protons are thus present in solution which competes with cadmium ions for cation exchange. As the pH of the solution increases, the acidity reduces hence there is a decrease in the number of protons available to compete with cadmium ions for cation exchange which resulted in a decrease in adsorption. Similar trend was observed by Dawodu *et al.* (2012) who study on the removal of cadmium (II) ions from aqueous solution by the use of "afuze" bentonite.

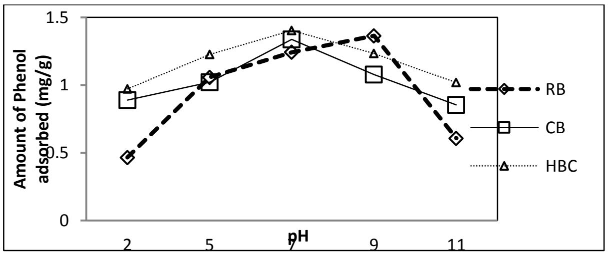

Fig. 5a: Effect of initial solution pH on aqueous phase adsorption of phenol on the adsorbents

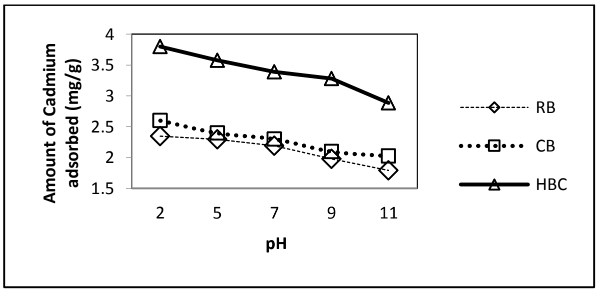

Fig. 5b: Effect of initial solution pH on aqueous phase adsorption of cadmium on the adsorbents

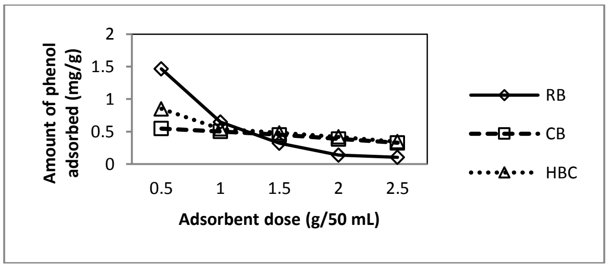

Fig. 6a: Effect of adsorbent dose on adsorption of phenol

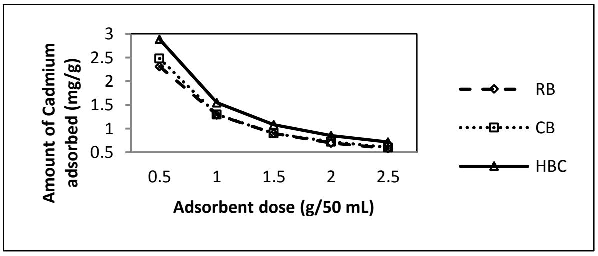

Fig. 6b: Effect of adsorbent dose on adsorption of cadmium

Effect of adsorbent dosage on phenol and cadmium uptake

Result in Fig. 6a for phenol shows that as the adsorbent dosage increases from 0.5 - 2.5 g for CB and HBC adsorption increased with increase in adsorbent dosage except for RB. Percentage removal showed that as the amount of adsorbent increases from 0.5 to 2.5 g, the percent removal of phenol increases from 21.912 - 65.504% for CB and 33.988 - 68.952% for HBC which may be due to increase in surface negative charges and decrease in the electrostatic potential near the solid surface that favors sorbent-solute interactions (Mohammad *et al.*, 2010), except for RB which decreases from 58.688 - 20.972% as the adsorbent dosage increased which may be due to overloading of the adsorbent on the adsorbate, resulting in low active surface area and the swelling nature of RB.

Similar trend was observed by Cowan and White (2001) for phenol. In the case of Cadmium in Fig. 6b it was observed that as the adsorbent dosage increases from 0.5– 2.5 g, that the percentage removal increased from 46.138 - 57.768 for RB, 49.628 - 59.970% for CB and 57.712 - 71.434% for HBC. The increasing trend in adsorption percentage as adsorbent dosage increases may be attributed to increase surface area and presence of additional available adsorption sites which leads to higher capacity for adsorption (Nanganoa *et al.*, 2014). Gandhi *et al.* (2012) who studied the kinetic and equilibrium modeling of the adsorption of amaranth from aqueous solution onto smectite clay observed the same trend. Comparatively, from their percentage removal it was observed that HBC gave a higher percentage values showing that they are better adsorbent to CB and RB.

Effect of the initial concentration on adsorption of phenol and cadmium

Figure 7 shows the effect of initial concentration adsorption of phenol and Cadmium. From Fig. 7a it was found that as the initial concentration of phenol increases from 5 - 25 mg /L, the amount of phenol adsorbed in (mg/g) increases from 0.199 - 1.287 mg/g for RB, 0.284 - 1.393 mg/g for CB and 0.304 - 1.563 mg/g for HBC respectively. From the result it is evident that at high concentration, the available sites of adsorption become fewer, which connected with the competitive diffusion process of the phenol through the micro-channel and pores in bentonite (Nassef and Eltaweel, 2012).

In the case of Cadmium in Fig. 7b similar trend is observed which shows that as the initial concentration of Cadmium increases from 10 – 50 mg/L that the amount of Cadmium increases from 0.290 - 2.091 mg/g for RB, 0.290 - 2.200 mg/g for CB and 0.479 - 2.410 mg/g for HBC. At lower concentrations, a large number of adsorption sites of adsorbents available to the Cadmium but increase concentration leads to strong competition for adsorption sites (Bhattacharyya and Gupta, 2011; Jiang *et al.*, 2011). Under these circumstances, the unit mass of the adsorbent could take up many more cadmium ions compared to that at lower concentrations. Similar observation for Cu (II) ions uptake on different sorbents have been reported by Bayat (2002). From the values it is evident that HBC are more potent adsorbent than the RB and CB which may be attributed to their porosity and high surface area (Ajay *et al.*, 2015).

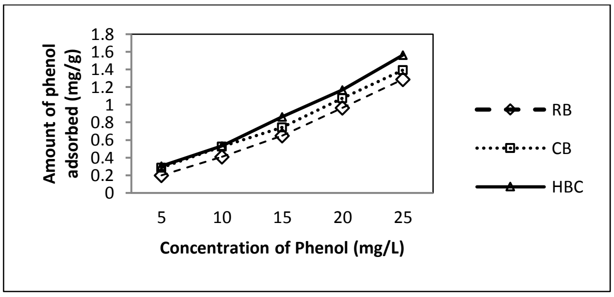

Fig. 7a: Effect of the initial concentration on adsorption of phenol

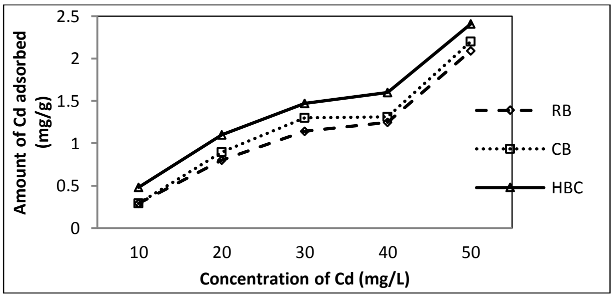

Fig. 7b: Effect of the initial concentration on adsorption of cadmium

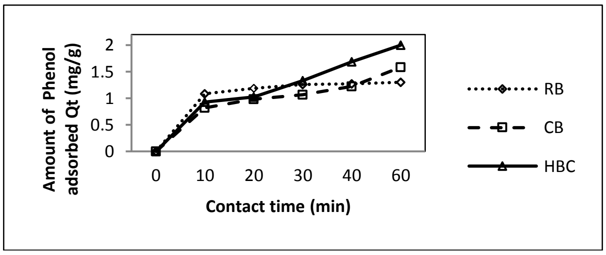

Fig. 9a: Effect of contact time on phenol uptake by adsorbent

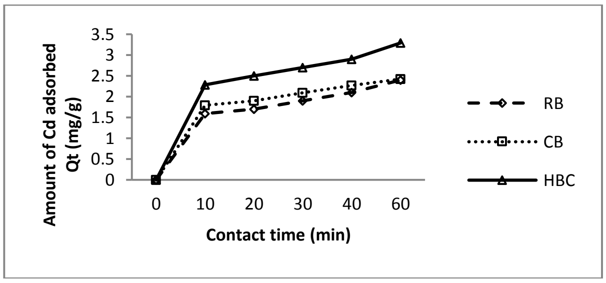

Fig. 9b: Effect of contact time on Cd uptake by adsorbent

Effect of contact time

Results in Figs 9a and 9b for phenol and Cadmium, shows that adsorption capacity increased at all times from (10 - 60 min) until equilibrium was attained at 60 min. The highest adsorption capacity of 1.301, 1.587, 1.999 mg/g were observed for RB, CB and HBC, respectively for phenol all at 60 min.

Similarly the highest adsorption capacity of 2.399, 2.420 and 3.292 mg/g was observed for RB, CB and HBC, respectively for Cadmium all at 60 min. This increase could be explained to the fact that, the ions adsorbed, occupied the active sites on the adsorbent which as the contact time increased the active sites on the sorbent became saturated (Bhattacharyya and Gupta, 2011). This is also in agreement with Ahmed *et al.* (2015) who studied on the Characterization and application of kaolinite clay as solid phase extractor for removal of copper ions from environmental water samples.

Comparatively, the removal capacity of CB is higher than RB, while HBC is higher than the CB for both phenol and Cadmium. This suggests that HBC is a more potent adsorbent as compared with others.

Adsorption kinetic model

Using Data obtained from the effect of contact time, the result from the kinetic parameters in Tables 4 and Figs. 10a-b show that the adsorption of phenol and cadmium on RB, CB and HBC could be described by both first and second order model. Based on correlation coefficient R^2, it was observed that the Blanchard pseudo-second order gave a better fit closer to unity for both phenol and Cadmium with R^2 values ranging from 0.906 - 0.999 for phenol and 0.981 - 0.995 for Cadmium as compared with the Lagergren pseudo-first order which gave lower R^2 values for both phenol and Cadmium on all the adsorbents in the range of 0.885 – 0.984 and 0.928 – 0.984, respectively and the pseudo-second order rate constants K_1 were in the range 0.012 – 0.543 g.mg^{-1}min^{-1} for phenol and 0.033 – 0.056 g.mg^{-1}min^{-1} for cadmium.

The high value of regression coefficient for the second - order shows that the pseudo second order equation best describes the entire adsorption process (Ahmed *et al.,* 2015). This shows that adsorption on all adsorbents may occur through a chemical process involving the valence forces of the shared or exchanged electrons which shows that chemisorption reaction or an activated process becomes more predominant in the rate-controlling step for the system (Ajay *et al.*, 2015). The kinetic data of phenol and cadmium onto RB, CB and HBC, were well presented by the Blanchard pseudo-second order suggesting that adsorption of cadmium was more favorable than phenol for CB, and HBC except for RB.

Table 4: Kinetic parameter for adsorption of phenol and cadmium on RB, CB and HBC adsorbents

Adsorbate	Model	Adsorbent		
		RB	**CB**	**HBC**
Phenol	**First order**			
	K_1 (Lmin^{-1})	0.071	0.024	0.041
	Qe (mg/g)	0.436	0.995	1.886
	R^2	0.984	0.974	0.885
Phenol	Second order			
	K_2 (g.mg^{-1}min^{-1})	0.543	0.026	0.012
	Qe (mg/g)	1.358	1.972	2.878
	R^2	0.999	0.930	0.906
	h (gmg^{-1}min^{-1})	0.100	0.100	0.099
Cadmium	**First order**			
	K_1 (Lmin^{-1})	0.033	0.048	0.031
	Qe (mg/g)	1.229	1.172	1.429
	R^2	0.939	0.928	0.984
Cadmium	Second order			
	K_2 (g.mg^{-1}min^{-1})	0.035	0.056	0.033
	Qe (mg/g)	2.732	2.656	3.643
	R^2	0.981	0.995	0.988
	h (gmg^{-1}min^{-1})	0.258	0.396	0.432

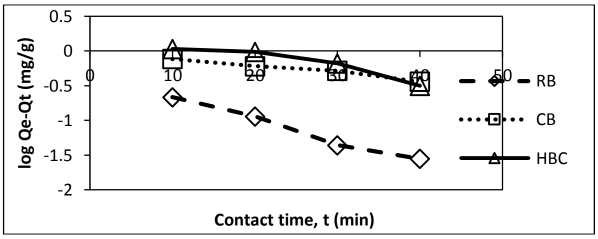

Fig. 10a: Lagergren pseudo-first order kinetic plots for adsorbent on phenol

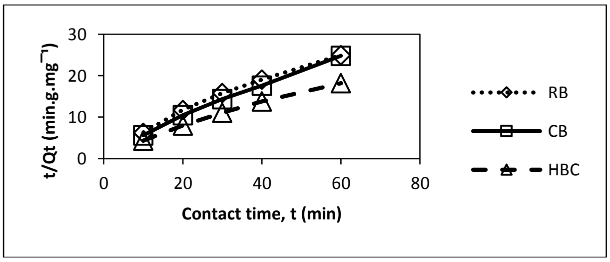

Fig. 10b: Blanchard pseudo-second order kinetic plots for the different adsorbent on cadmium

Freundlich isotherm model for adsorption of phenol and cadmium

The linearized form of Freundlich equation as stated earlier in equation 3. The value of K_F and n_F are obtained from slope and intercept of the plot of log Q_e versus log C_e. Freundlich assumes that adsorption takes place on heterogeneous surface of the adsorbent (Nanganoa *et al.,* 2014). From the Freundlich model results in Table 5 for phenol, a high K_F value of (0.139) was obtained for HBC, than the RB and CB suggesting that HBC has good capacity for adsorbing phenol (Krishna and Swamy, 2012).

A similar trend was observed for Cadmium with values of (0.138) suggesting HBC as better adsorbent which may be attributed to their porosity and high conductivity as well (Bousba and Meniai, 2013). The adsorption intensity n_F from Table 5 also shows that adsorption is favourable for values greater than 1 and less than 1 as unfavourable (Dawodu *et al.*, 2012). The lesser R^2 values obtained from the regression equation for Freundlich isotherm suggests that the adsorption is homogenous rather than heterogeneous (Nanganoa *et al.*, 2014). The 1/n values were found to be above 1 is an indication that the adsorption is unfavourable while those with values of 0-1 range shows fovourable adsorption for both phenol and Cadmium. This is in agreement with Bousba and Meniai (2013) who studied on the Adsorption of 2-Chlorophenol onto Sewage Sludge based Adsorbent.

Table 5: Isotherm parameters for phenol and cadmium adsorption on adsorbents

Adsorbate	Model	Adsorbent		
		RB	CB	HBC
Phenol	**Langmuir**			
	Q_m(mg/g)	1.895	4.314	6.042
	b (L/mg)	0.032	0.032	0.032
	R^2	0.997	0.983	0.961
	R_L	0.860	0.862	0.862
Phenol	**Freundlich**			
	1/n	1.316	0.938	1.011
	n_F	0.760	1.066	0.989
	R^2	0.982	0.971	0.951
	K_F((mg/g) L/mg)1/n)	0.043	0.130	0.139
Cadmium	**Langmuir**			
	Q_m(mg/g)	2.303	1.764	25.316
	b (L/mg)	0.017	0.022	0.004
	R^2	0.935	0.877	0.943
	R_L	0.855	0.820	0.962
Cadmium	**Freundlich**			
	1/n	1.181	1.187	0.846
	n_F	0.847	0.843	1.183
	R^2	0.908	0.846	0.903
	K_F((mg/g) L/mg)1/n)	0.030	0.037	0.138

Adsorption Isotherm Models

Langmuir isotherms model for adsorption of phenol and cadmium

On the assumption that adsorption occurs at homogeneous sites and forms a monolayer, Langmuir models are used (Nanganoa *et al.*, 2014). The langmuir theoretical constants Q_m and K_L were calculated from the slope and intercept of a linear plot of 1/Qe versus 1/Ce, respectively.

From the results in Table 5, for phenol, the maximum adsorption capacity, Q_m for phenol gave values of (1.895, 4.314, 6.042 mg/g) for RB, CB and HBC, respectively.

Similarly results for Cadmium in Table 5, gave values of (2.303 mg/g, 1.764 mg/g, 25.316 mg/g) for RB, CB and HBC, respectively. These values represents, the total number of binding sites that are available for adsorption for each adsorbents (Tan *et al.*, 2009). The high value of HBC (6.042 mg/g) for phenol and (25.316 mg/g) for Cadmium is an indication that HBC has high number of total binding sites for adsorption of phenol and Cadmium than their corresponding RB and CB which may be attributed to their porosity and high conductivity (Ajay *et al.*, 2015). From the characteristics of the langmuir isotherm determined from thre experimental data by the dimensionless constant called separation factor, R_L, the values were all < 1 and > 0 indicating that adsorption is favourable for all adsorbent (Krishna and Swamy, 2012). From the results based on correlation coefficients R^2 on the adsorption of Phenol and Cadmium as described by both Langmuir and Freundlich isotherms in Table 5. The Langmuir gave the highest R^2 value of (0.997) for phenol and (0.943) for Cadmium as compared with Freundlich which gave (0.982) for phenol and (0.917) for Cadmium. This showed that the experimental data best obeyed the Langmuir isotherm, than the Freundlich for both Phenol and Cadmium. This means that the Langmuir model best described the experimental data. Based on this model, it can be concluded that the active sites on the adsorbents surface were distributed in homogeneous form, and monolayer adsorption manner was dominant in the adsorption of Phenol and Cadmium (Bai *et al.*, 2010).

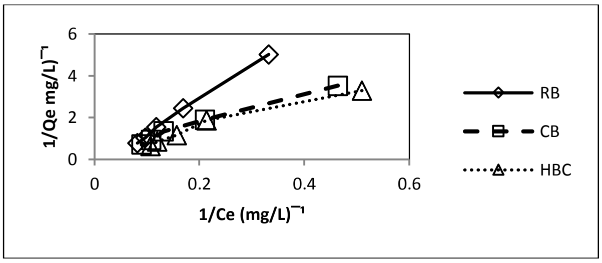

Fig. 11a: Langmuir isotherm for phenol

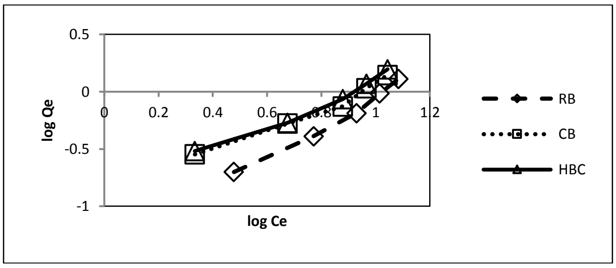

Fig. 11b: Freundlich isotherm for phenol

Thermodynamic parameter for adsorption of phenol and cadmium

Thermodynamics is an important parameter that determines the spontaneity of the adsorption process (Tan *et al.*, 2012). Table 6, shows the calculated values of thermodynamic parameters.

From the Table, it is observed that the values of ΔH^0 are all positive for phenol and Cadmium ranging from (23.271–40.378 kJmol^{-1}) and (11.025 - 12.704 kJmol^{-1}), respectively. This is an indication that endothermic reaction of adsorption process dominate, hence chemisorption dominates physisorption (Bai *et al.*, 2010). Similar observation and explanation have been given Gupta and Nayak (2011) studies on Cadmium removal and recovery from aqueous solutions by novel adsorbents prepared from orange peel and Fe_2O_3 nanoparticles.

Table 6: Thermodynamic parameters of adsorption for phenol and cadmium

Adsorbate	Adsorbents	ΔH(kJ/mol x1000)	ΔS(kJ/ molK)	R^2	ΔG(kJ/mol x1000)
Phenol	RB	23.271	67.331	0.996	1.186
	CB	25.414	64.796	0.9991	4.161
	HBC	40.378	115.455	0.994	2.508
Cadmium	RB	12.704	22.643	0.673	5.504
	CB	11.477	20.528	0.630	4.949
	HBC	11.025	20.082	0.929	4.639

The high positive values of ΔS^0, ranging from 64. 796 – 115.455 kJ/molK and 20.082 – 22.643 kJ/molK for phenol and cadmium, is attributed to high degree of disorder at the solid- liquid interface during adsorption processes (Tan *et al.*, 2012).

The positive value of Gibbs free energy ΔG^0 for phenol ranging from (1.186 – 4.161 kJ/mol) and (4.639 – 5.504 kJ/mol) for phenol and cadmium is an indication that the reaction is not spontaneous in nature (Jameel *et al.*, 2012). According to Dula *et al.*, (2014) values from (80- 400 kJmol^{-1}) indicate that chemisorption dominates physisorption.

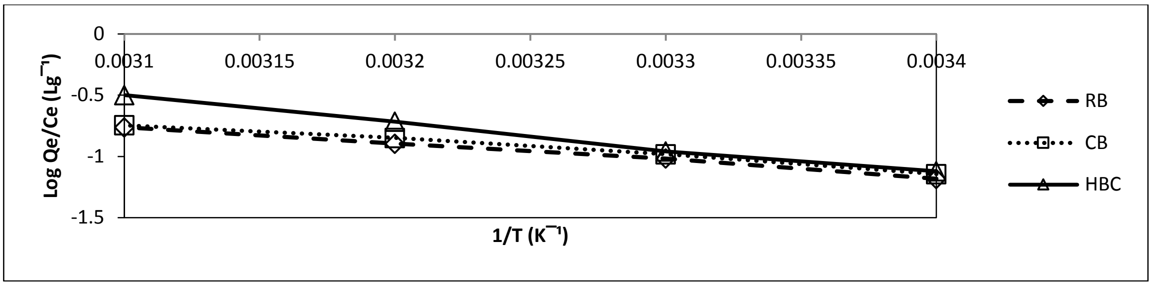

Fig. 12a: Van't Hoff Plots for adsorption of phenol

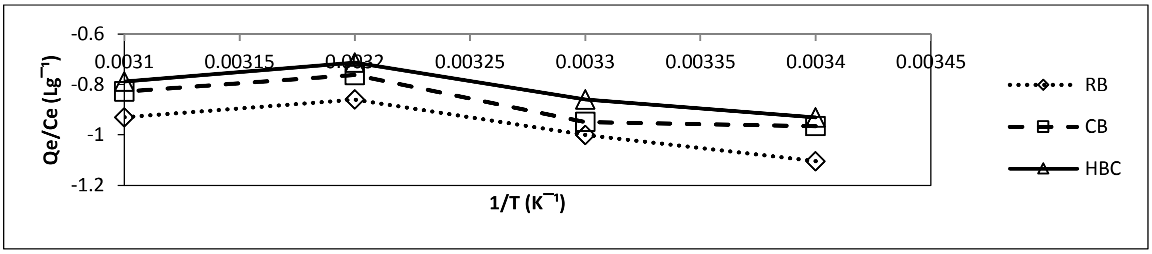

Fig. 12b: Van't Hoff plots for adsorption of cadmium

Conclusion

Adsorbents such as Raw Bentonite (RB), Carbonized (CB) and Hydroxyiron (III) -Bentonite Composite (HBC) exhibited good physicochemical attributes.

Based on the investigation phenol and cadmium uptake are strongly affected by initial solution pH, initial solution concentrations, adsorbent dosage, temperature and time of contact. Adsorption capacity of phenol was found to decrease with increase in adsorbent dose for CB, HBC except for RB which increases with increase in adsorbents dose. While Adsorption capacity of cadmium was found to decrease with increase in adsorbent dosage for RB, CB and HBC. The optimum pH for adsorption of phenol was found to be pH 7-9 while that of cadmium was found to be pH 2.

For the experimental data for phenol and cadmium, it was found that data fitted the linearized Langmuir isotherm better than the Freundlich isotherm indicating that the adsorption is monolayer. On the effect of initial solution concentration, adsorption capacity of phenol and cadmium was found to increase with increase in concentration for RB, CB and HBC. Adsorption capacity of phenol increases with increase in temperature for RB, CB and HBC except for cadmium which increases initially and then decreases after attaining saturation, suggesting a non-spontaneous and endothermic sorption process. Kinetic data was fitted into pseudo second order model than first order suggesting that chemisorption dominate the rate limiting step.

References

Abdus-Salam N & Buhari M 2014. Adsorption of Alizarin and Fluorescein Dyes on Adsorbent prepared from Mango Seed. *Pacific J. Sci. & Tech.*, 15(1): 232-244.

Afaj HA, Mohammad RM & Mahmoud NM 2015. Removal of phenol from industrial effluents using activated carbon and Iraqi Porcelanite rocks – A comparative study. *J. Ministry of Sci. & Techn*., 91: 21-32.

Ahmed AS, Tantawy AM, Abdallah ME & Qassim IM 2015. Characterization and application of kaolinite clay as solid phase extractor for removal of copper ions from environmental water samples. *Int. J. Advanced Res.*, 3(3): 1-21.

Ahmedna M, Marshall WE & Rao RM 2000. Production of granular activated carbon from select agricultural by-products and evaluation of their physical, chemical, and adsorptive properties. *Bioresource Technology*, 71(2): 113-123.

Ajay KA, Mahendra SK, Chandrashekhar PP & Ishwardas LM, 2015. Kinetics study on the adsorption of ni^{2+} ions onto fly ash. *J. Chem. Techn. & Metallurgy,* 50(5): 601-605.

Alinnor IJ & Nwachukwu MA 2012. Adsorption of phenol on surface – modified cassava peel from its aqueous solution. *Int. J. Envtal. Sci., Mgt. & Engr. Res.*, 1(2): 68-76.

Arellano-C´ardenas S, Gallardo-Vel´azquez T, Osorio-Revilla G, L´opez-Cort´ez Ma del S & G´omez-Perea B 2005. Adsorption of phenol and dichlorophenols from aqueous solutions by porous clay heterostructure (PCH). *J. Mexican Chem. Soc.*, 49: 287-291.

Arias F & Sen TK 2009. Removal of zinc metal ion (Zn^{2+}) from its aqueous solution by kaolin clay mineral: A kinetic and equilibrium study. *Colloid Surface Journal*, 348: 100–108.

Aroke U OL, El-NafatyUA & Osha OA 2013. Properties and characterization of kaolin clay from alkaleri, North-Eastern Nigeria. *Int. J. Emerging Techn. & Advanced Engr.*, 3(11): 387-392.

Bai TM, Komali K & Ventakeswarhi P 2010. Equilibrium, kinetics and thermodynamic studies on biosorption of copper and Zinc from mixed solution by Erythrina *Variegata orientalis* leaf powder. *India J. Chem. Techn*., 17: 346-355.

Bansal RC & Goyal M 2005. Activated carbon adsorption. Boca Raton, Crc press Taylor and francis group. 6000 broken sound parkway NW, suite 300 Boca Raton, FL, USA, pp. 33487-2742.

Bansode RR 2002. Treatment of Organic and Inorganic Pollutants in Municipal Wastewater by Agricultural by-product based Granular Activated Carbon (GAC). Unpublished M.Sc. Thesis. Louisiana State University and Agricultural and Mechanical College: Alexandria, LA.

Bayat B 2002. Comparative study of adsorption properties of Turkish fly ashes I. The case of nickel(II), copper(II) and zinc(II). *J. Hazard. Material,* 95: 251–273.

Bhattacharyya KG & Gupta SS 2011. Removal of Cu (II) by natural and acid-activated clays: an insight of adsorption isotherm, kinetics and thermodynamics. *Desalination*, 272: 66–75.

Bhattacharyya KG, SenGupta S & Sarma GK 2014. Interactions of the dye, rhodamine B with kaolinite and montmorillonite in water. *Appl. Clay Sci*., 99: 7–17.

Bhole BD, Ganguly B & Madhuram A 2004. Biosorption of Methyl Violet, Basic Fuschin and Their Mixture Using

Dead Fungal Biomass. *Research Communications*, 86: 1641-1645.

Bolat F, Govori S, Haziri A, Spahiu S & Faiku F 2010. Used tea waste adsorption for removal of phenol from synthetic and Kosovo Industrial waste water. *Int. J., Envtal. Application & Sci.*, 1: 63-67.

Bousba S & Meniai HA 2013. Adsorption of 2-chlorophenol onto sewage sludge based adsorbent: Equilibrium and kinetic study. *Chemiical Engiineeriing Transactiions*, 35: 859-864.

Chen X 2015. Modeling of experimental adsorption isotherm data. *Open Access Information*, 6: 14-22.

Cowan CT & White D 2001. Adsorption by Organo-Clay Complexes",Ninth National Clay and Clay Mineral Conference.

Dawodu FA, Akpomie GK & Ogbu I 2012. The removal of cadmium (ii) ions from aqueous solution by the use of “afuze” bentonite: Equilibrium, kinetic and thermodynamic studies. *Int. J. Scientific & Engr. Res.*, 3(12): 1 – 8.

Denizli A, Ozkan G & Ucar M 2001. Removal of chlorophenols from aquatic systems with dye affinity microbeads. *Separation & Purification Tech.*, 24(1-2): 255–262.

Dula T, Siraj K & Kitte SA 2014. Asdorption of hexavalent chromium from aqueous solution using chemically activated carbon prepared from locally available waste of bamboo. *Int. Scholarly Res. Notices in Envtal. Chemistry*, 1-10.

El-Dars ESMF, Ibrahim MH, Farag BAH, Abdelwahhab ZM & Shalabi HEM 2016. Preparation, characterization of bentonite carbon composite and design application in adsorption of bromothymol blue dye. *J. Multidis. Engr. Sci. & Techn.*, 3(1): 3758-3765.

Essomba SJ, Ndi Nsami J, Belibi Belibi BP, Tagne MG & Ketcha Mbadcam J 2014. Adsorption of cadmium(II) ions from aqueous solution onto kaolinite and metakaolinite. *J., Pure & Appl. Chem. Sci.*, 2(1): 11 – 30.

Faye G, Bekele W & Fernandez N 2014. Removal of nitrate ion from aqueous solution by modified Ethiopian bentonite clay. *Int. J. Res. Pharmacy & Chem.*, 4(1): 192-201.

Gandhi NL, Sirisha DL, Asthana S, Manjusha A 2012. Adsorption studies of fluoride on *Multani matti* and red soil. *Resources J.Chem. Sci*., 2(10): 32-37.

Gupta, K.V and Nayak, A (2011). Cadmium removal and recovery from aqueous solutions by novel adsorbents prepared from orange peel and Fe_2O_3 nanoparticles. *Chemical Engineering Journal*, 180: 81-90.

Jameel MD, Hussien AK & Nasser T 2012. Removal of cadmium ions from industrial wastewater Using Iraqi *Ceratophyllum demersum*. *Al- Mustansiriyah Journal Sci.*, 32(8): 71-84.

Jiang M, Jin X, Lu X & Chen Z 2011. Adsorption of Pb(II), Cd(II), Ni(II) and Cu(II) onto natural kaolinite clay. *Desalination*, 252:33–39.

Johari K, Saman N, Song ST, Heng JYY & Mat H 2014. Study of Hg(II) removal from aqueous solution using lignocellulosic coconut fiber biosorbents. *Equilibrium & Kinetic Evaluation*, 1198-1220.

Karapinar N & Donat R 2009. Adsorption behavior of Cu^{2+} and Cd^{2+} onto natural bentonite. *Desalination*, 249: 123-129.

Kibami D, Pongener C, Rao KS & Sinha D 2014. Preparation and characterization of activated carbon from *Fagopyrum esculentum* Moench by HNO_3 and H_3PO_4 chemical activation. *Der Chemica Sinica*. 5(4):46-55

Kosmulski MJ 2009. *J. Colloid & Interface Science*, 337: 439–448.

Krishna HR & Swamy SVVA 2012. Physico-chemical key parameters, Langmuir and Freundlich isotherm and Lagergren rate constant studies on the removal of divalent nickel from the aqueous solutions onto powder of calcined brick. *Int. J. Engr. Res. & Devt.*, 4(1): 29-38.

Li X, Cui Y & Femg Y 2005. Reaction pathways and mechanisms of the electrochemical degradation of phenol on different electrodes. *J. Water Research*, 39(10): 1972-1981.

Liew YM, Kamarudin H, Mustafa AL, Bakri AM, Luqman M, KhairulNizar I, Ruzaidi CM & Heah CY 2012. Processing and characterization of calcined kaolin cement powder. *Constr. Build. Material journal, 30: 794–802.*

Makeswari M, Santhi T & Ezhilarasi MR 2016. Adsorption of methylene blue dye by citric acid modified leaves of Ricinus communis from aqueous solutions. *J. Chem. & Pharmac. Res*., 8(7): 452-462.

Mohammad WA, Fawwaz IK & Akl AM 2010. Adsorption of lead, zinc and cadmium ions on polyphosphate-modified kaolinite clay. *J. Envtal. Chem. & Ecotoxic.*,2(1): 001-008.

Mohanty K, Das D, Biswas MN 2005. Adsorption of phenol from aqueous solutions using activated carbons prepared from Tectona grandis sawdust by $ZnCl_2$ activation. *Chem. Engin. Journal*, 115(1- 2): 121–31.

Moradi M, Dehpahlavan A, Kalantary RR, Ameri A, Farzadkia M & Izanloo H 2015. Application of modified bentonite using sulfuric acid for the removal of hexavalent chromium from aqueous solutions. *Envtal. Health Engr. & Mgt. J.*, 2(3): 99–106.

Nanganoa LT, Ketcha JM & Ndi JN 2014. Kinetic and equilibrium modeling of the adsorption of Amaranth from aqueous solution onto Smectite Clay. *Res. J. Chem. Sci.*, 4(2): 7-14.

Nassef E & Eltaweel Y 2012. Adsorption of phenol from aqueous solutions by local egyptian bentonite. *Journal of American Science*, 8(8): 581-589.

Naswir M, Arita S, Marsi & Salni 2013. Characterization of bentonite by XRD and SEM-EDS and use to increase pH and color removal, Fe and Organic Substances in Peat Water, 1(4): 313-317.

Okieimen CO & Okieimen FE 2001. Enhanced metal sorption by groundnut (arachis hypogea) husks modified with thioglycollic acid. *Bull. Pure Appl. Sci.*, 20c: 13-20.

Rao PS, Kalyani S, Reddy KVNS & Krishnaiah A 2011. Comparison of biosorption of nickel(II) and copper(II) ions from aqueous solution by sphaeroplea algae and acid treated *Sphaeroplea algae*. *Sep. Sci. Technol*., 40: 3149–3165.

Srivastava R, Upreti RK, SR, Prasad KN, Seth PK & Chaturvedi UC 2006. Suboptimal chlorine treatment of drinking water leads to selection of multidrug-resistant *Pseudomonas aeruginosa*. *Ecotoxicology & Environmental Saftety*, 58(2): 277-283.

Syafalni Abdullah R, Abustan I & Ibrahim MNA 2013. Wastewater treatment using bentonite, the combinations of bentonite-zeolite, bentonite-alum, and bentonite-limestone as adsorbent and coagulant. *Int. J. Environmental Sci.*, 4(3):379-391.

Tan J, Zhang X, Wei X & Wang L 2012. Basic dye ssorption on ONP fiber. *Bio. Resources*, 7(3): 4307-4320.

Toles CA, Marshall WE, Johns MM, Wartelle LA & McAloon A 2000. Acid activated carbons from almond shells: Physical, chemical and adsorptive properties and estimated cost of production. *Bioresource Technology*, 71: 87-92.